HHS Public Access

Author manuscript

J Vasc Interv Radiol. Author manuscript; available in PMC 2018 July 01.

Published in final edited form as:

J Vasc Interv Radiol. 2017 July ; 28(7): 1043–1050.e2. doi:10.1016/j.jvir.2017.03.037.

Relative initial weight is associated with improved survival without altering tumor latency in a translational rat model of diethylnitrosamine-induced hepatocellular carcinoma and transarterial embolization

Ryan M. Kiefer[1], **Stephen J. Hunt**[1,2], **Santiago Pulido**[1], **Stephen Pickup**[2], **Emma E. Furth**[3], **Michael C. Soulen**[2], **Gregory J. Nadolski**[1,2], and **Terence P. F. Gade**[1,2]

[1]Penn Image-Guided Interventions Laboratory, University of Pennsy Philadelphia, PA 19104

[2]Department of Radiology, Perelman School of Medicine at the University of Pennsylvania, Philadelphia, PA 19104

[3]Department of Pathology and Laboratory Medicine, Perelman School of Medicine at the University of Pennsylvania, Philadelphia, PA 19104

Abstract

Purpose—To test the hypotheses that greater initial body weight is associated with a relative improvement in survival with diminished fibrosis in a diethylnitrosamine (DEN)-induced rat model of HCC and that TAE (TAE) via femoral artery access decreases procedure times compared to carotid artery access.

Materials and Methods—138 male Wistar rats were administered 0.01% DEN in water *ad libitum* for 12 weeks. Rats received weekly T2-MRI to detect HCC. Upon development of ≥5mm tumors, rats underwent selective TAE via carotid or femoral artery catheterization under fluoroscopic guidance. Rats were retrospectively categorized into 3 groups (<300g, 300-400g, >400g) based on initial weight for analyses of survival, tumor latency, and fibrosis. Site of access was compared relative to procedural outcomes of success, mortality, and time.

Results—No significant differences in tumor latency were related to weight group (p=0.310). Rats weighing <300g had shorter survival time than both larger groups (mean=88d vs. 108d, p<0.0001) and more severe fibrosis (<300g median=4.0, 300-400g median=1.5, >400g median=1.0; p=0.015). No significant difference was found in peri-procedural mortality based on access site; however, procedure times were shorter via a femoral approach (mean=71+/-23min vs. 127+/-24min; p<0.0001).

Conclusion—Greater initial body weight resulted in improved survival without prolonging tumor latency for rats with DEN-induced HCCs and was associated with less severe fibrosis. A femoral approach for TAE in this model resulted in decreased procedure time. These modifications

Corresponding Author: Terence P. F. Gade, MD, PhD, Assistant Professor of Radiology, Department of Radiology, Division of Interventional Radiology, Hospital of University of Pennsylvania, 3400 Spruce Street, Philadelphia, PA 19104, Terence.Gade@uphs.upenn.edu, Phone: 215-573-9756.

Accepted for oral presentation at SIR Annual Scientific Meeting 2017

provide a translational animal model of HCC and TAE that may be suited for short-term survival studies.

Keywords

diethylnitrosamine; transarterial embolization; hepatocellular carcinoma; animal models; interventional oncology

Introduction

Given that a minority of patients with hepatocellular carcinoma (HCC) present with resectable disease, locoregional therapies such as transarterial chemoembolization/TAE (TACE/TAE) provide important means of tumor suppression and can improve survival (1–3). Although long-term survival remains low owing to recurrence and de novo tumor growth, developments in cancer biology hold promise for increasing the effectiveness of endovascular techniques through molecular and cell-based therapies (4–6). In order to advance these therapies toward clinical trials, translational animal models that recapitulate the complexity of human disease and mitigate the challenges of endovascular interventions must be developed.

Currently, a number of animal models of HCC exist, and each has been purported to offer unique benefits. Small animal models typically carry lower costs than large animal models, but until recently had been thought too small to allow for selective endovascular treatments (7). Xenograft models of HCC allow for reproducible tumors that are easily detected with short latencies, but fail to accurately recreate the tumor microenvironment of underlying liver injury that characterizes human disease (8–11). Similarly, orthotopic tumor models lack the phenotypic background of cirrhosis as well as the arterial dependence of HCC that characterizes human pathogenesis. These features can be reproduced using autochthonous models such as the chemically-induced diethylnitrosamine (DEN) model (8,12,13).

Segmental TAE in a DEN-induced rat model of HCC has previously been described (7). Two limitations we sought to address from that model were the length and complexity of the procedure and the short survival window post tumor induction. Prior reports describe TAE via laparotomy or carotid arterial access (7,10,14,15). Femoral access has been successfully demonstrated as a feasible approach for hepatic angiography in a rat, but embolization outcomes have not been reported (16,17). Dose-dependent liver injury has been demonstrated in the DEN-induced rat model with controlled drug delivery via gastric gavage, however this method is resource intensive (18,19). Prior research has found that *ad libitum* mammalian water consumption is inversely related to body weight (20,21). As such, animals with larger body weight would be predicted to consume less toxin relative to body weight and theoretically develop less severe cirrhosis. In this study of a DEN-induced rat model of HCC, we hypothesized that rats with larger initial weight would have lower cirrhotic disease burden and increased survival and that a femoral artery approach to TAE would produce more favorable treatment parameters when compared to a carotid artery approach.

Materials and Methods

Complete experimental details, are located in the Supplementary Materials & Methods section.

Animal Model

Institutional animal care and use committee approval was granted prior to the start of the experiment. One hundred thirty-eight (138) male Wistar rats (Charles River Laboratories International, Inc., Wilmington, Massachusetts) were acclimated to the animal facility for 2 weeks prior to administration of *ad libitum* 0.01% DEN (Sigma-Aldrich, St. Louis, Missouri) in water for 12 weeks.

Rats were retrospectively assigned to weight cohorts based on their body weight at the initiation of the diet. The cutoff value for weight cohorts was determined to ensure that each cohort demonstrated commensurate growth based on published growth curves in order to limit confounding effects of growth (22). The <300g group (approximate age 5-7 weeks) consisted of 70 rats weighing an average of 151g (range 115-183g) at the start of the DEN diet. Of note, data from a portion of the <300g group has been previously analyzed and presented separately from the analyses provided in this study (7). The 300-400g group (approximate age 7-11 weeks) consisted of 23 rats weighing an average of 354g (range 301-392g) at the start of the diet. The >400g group (approximate age 9-15 weeks) had 45 rats weighing an average of 442g (range 403-490g) at the start of the diet. All data from the 300-400g and >400g groups are unique to this study. Sixteen (16) rats in the <300g group died prior to completing the diet and two (2) rats from the >400g group were removed from the diet due to lethargy and were later restarted, but were not included in statistical analyses of tumor latency or survival due to the interruption in treatment. Eleven (11) rats had inexact dates of death and were excluded. A total of 125 rats with exact documented dates of death or procedure were used for survival analysis. For analyses of cohort weight gain, rat weights were averaged within weight groups for each day of the diet. A cohort of 26 rats housed individually or together with another rat was used to analyze the influence of cohabitation on *ad libitum* DEN water intake. To record DEN intake, water bottles were weighed to track consumption throughout the diet. For rats under paired housing conditions, the total water consumption was averaged between the two rats.

Magnetic Resonance Imaging

Within the first three days of completing the DEN diet, rats underwent initial T2-weighted MRI to monitor for tumor initiation and growth. Thereafter, weekly MRI was performed until rats were found to have at least 1 tumor measuring ≥5mm as described previously(7).

TAE

After the development of radiographically-evident ≥5mm HCC tumors, 34 rats were scheduled to undergo TAE (TAE). Some rats that developed HCC died prior to being embolized and others were allocated for use in a parallel study (Table 1). TAE of HCC tumors was performed under fluoroscopic guidance using an AngioStar Plus Imaging System (Siemens, Malvern, Pennsylvania) via a left common carotid or right common

femoral artery approach. The first 13 rats treated were all from the <300g group and were embolized by carotid approach while the later cohort consisted of 21 rats in the 300-400g and >400g groups and were treated via femoral approach. Procedures were performed under inhaled anesthesia with 2% isoflurane administered through a nose cone with body temperature monitored using a rectal probe and maintained at 37°C using a circulating warm water heating pad. Embolization technique via carotid artery approach has been previously reported (7). For the femoral artery approach, the rat was placed in a supine position. Using stereomicroscopy (Leica Microsystems AG, Heerbrugg, Switzerland) under 30× magnification, an arteriotomy was made in the right common femoral artery using a 26 gauge needle. A 9-0 monofilament suture was placed in the proximal lip of the arteriotomy to facilitate cannulation and closure. The artery was cannulated using a 1.5F microcatheter (Excelsior SL-10 Microcatheter, Stryker, Kalamazoo, Michigan) modified to 30cm while using blunt forceps and back-tension with the above described 9-0 suture. After cannulation, a hydrophilic-coated 0.014 inch diameter guidewire (Transcend guidewire, Stryker, Kalamazoo, Michigan) was introduced through the catheter to aid selection of the celiac artery. Celiac arteriography was obtained using iopamidol contrast (Isovue 370, Bracco Diagnostics, Inc., Monroe Township, New Jersey). Superselective cannulation of the segmental artery supplying the tumor and embolization was then performed (Embospheres, Merit Medical Systems, South Jordan, UT; 40-120 μm, 0.1 mL). Post-embolization digital subtraction angiography was then performed. After removal of the catheter, the arteriotomy was closed with 9-0 suture and the fascia and skin were closed using an interrupted suture pattern with 5-0 monofilament suture. Each rat was monitored during recovery from anesthesia and on the day following the procedure to evaluate for any signs of distress and then subsequently evaluated every other day.

Tissue Collection and Histology

Rats that did not expire were euthanized 12 days after embolization using inhaled carbon dioxide to enable tissue analysis for a parallel study based on our prior experience demonstrating a median post-procedure survival of 12 days (7). Partial necropsy was immediately performed after expiration or euthanasia, and both tumor and non-tumorous liver tissues were collected for staining and evaluation. Hematoxylin & eosin (H&E) and Masson trichrome staining were performed on tissue samples using standard protocols. Tissues were evaluated by a gastrointestinal pathologist (EEF) with extensive experience (>25 years) in HCC evaluation for confirmation of malignancy and staging of fibrosis. Nineteen (19) rats with confirmed HCC were randomly selected for fibrosis staging and analysis according to the METAVIR scoring system (23).

Statistical Analysis

Statistical analyses were performed using GraphPad Prism 6.02 (GraphPad Software, San Diego, California).

Results

Animal Model Characterization

The animal model was characterized using 3 cohorts of rats grouped by weight, each of which were treated with 0.01% DEN-water *ad libitum*. Linear regression analyses demonstrated significant differences between the best-fit slopes of weight gain for all groups (<300g 2.26g/day, 300-400g 1.07g/day, >400g 0.87g/day; p<0.0001) (Figure 1). At the end of the diet, the <300g group had gained an average of 202g, the 300-400g group had gained an average of 74g, and the >400g group had gained an average of 60g. A significant difference was found in length of survival recorded from the start of the DEN diet when comparing the rats by weight group (Figure 2). The 300-400g (mean=108+/-11.0d, n=22) and >400g (mean=108+/-20.5d, n=42) groups survived longer than the <300g weight group (mean=88+/-26.2d, n=61) (p<0.0001). There was no significant difference found between the 300-400g group and >400g group for survival (p=0.594).

Seventy-seven rats underwent MRI and all 77 were found to develop radiographic evidence of HCC over the course of serial imaging. While irregular appearance of the hepatic contour as well as nodularity of the hepatic parenchyma were appreciated on MR imaging, quantification of these features was outside of the scope of this study. Twenty (20) of the imaged rats were excluded from tumor latency analysis because they were not imaged within the first week of completing the DEN diet. The overall average tumor latency for the remaining 57 rats was 98 days (range 84-146d) from the start of the DEN diet. No significant correlation was observed between tumor latency and initial body weight (p=0.826) and no significant difference in average tumor latency was detected between group cohorts (<300g mean=97+/-5.3d, n=9; 300-400g mean=102+/-13.9d, n=14; >400g mean=96+/-14.3d, n=34; p=0.310) (Figure 3). In order to further characterize the larger rats, DEN consumption for a cohort of 26 rats (392g-485g) housed individually (12 rats) or with a cage mate (14 rats) was recorded over the 12-week diet. The total average toxin consumption over the course of the diet was 0.260mL (range=0.219-0.328mL). Rats that were housed individually were found to consume significantly more DEN on average than rats housed in pairs (0.286+/-0.031mL vs. 0.240+/-0.014mL, respectively; p<0.0001), however, no significant differences in average tumor latency were detected with respect to housing (95+/-10.9d vs. 91+/-9.0d, p=0.377). Tumor latency was not significantly correlated to total relative DEN consumption when the 26 rats were analyzed together (p=0.370) or when they were separately analyzed by individual housing (p=0.281) or shared housing (p=0.360) (Supplemental Figure 1).

Histologic analysis confirmed the development of HCC in each rat. Further, treated tumors were found to contain broad regions of ischemic necrosis. Trichrome-staining of the non-tumor hepatic parenchyma was used to stage the fibrosis with the METAVIR scoring system (stage 0 to 4 [cirrhosis]) (23). Fibrosis ranged from grade 0 to grade 4 in this cohort, with a significant difference among overall weight groups (p=0.016) (Figure 4). Additional analyses found significantly more fibrosis in the <300g group (median=4.0) compared to both the 300-400g group (median=1.5, p=0.034) and >400g group (median=1.0, p=0.015),

with no significant difference of fibrosis stage found between the 300-400g and >400g groups (p=0.406).

TAE

A total of 34 rats underwent TAE for this study (Figure 5). Thirteen (13) rats were treated via left common carotid artery (CCA) approach and 21 rats were treated via right common femoral artery (CFA) approach. No vasospasm was appreciated on angiography in any of the treated animals. Technical success, defined as the ability to embolize a segmental hepatic arterial branch, was achieved in 10 rats treated via CCA approach and 20 rats treated via CFA approach (technical success rates 77% and 95%, respectively; p=0.274) (Table 2). One (1) rat from the group successfully undergoing CCA approach died in the first 24 hours following the procedure, and 2 rats successfully treated from the femoral approach group died in the peri-procedural period, likely secondary to nontarget embolization. No significant difference was observed in peri-procedural mortality between approaches (p=1.000); however, procedure time, recorded as time of opening incision to time of closure, was significantly less for the femoral artery approach (mean 71+/-23min vs. 127+/-24min; p<0.0001).

Discussion

The results of this study further characterize the hepatocarcinogen model of DEN-induced HCC and compare two approaches to TAE in a small animal model. With a large cohort of male Wistar rats, survival was found to be significantly longer for animals of larger weights at the time of DEN initiation, while tumor latency was not significantly different. Importantly, the underlying degree of fibrosis was significantly reduced in animals with larger weights at the time of DEN initiation. Additionally, selective transfemoral arterial embolization of HCCs was found to be as successful and as safe as a previously described carotid approach while requiring significantly less time to perform and more closely mimicking the procedural approach used in patients (7).

Autochthonous models of HCC are necessary for the study of potential molecular and cell-based therapies as these models induce alterations not only at the structural level but at the biochemical and genetic level needed to accurately assess response (8,18). While xenograft models allow for rapid induction of tumors and may be sufficient for some study designs, the complexities of HCC can only be fully appreciated with models that faithfully recapitulate tumorigenesis. Of the chemotoxic agents studied for use in hepatocarcinogenesis, DEN has a number of advantages including the demonstrated ability to produce phenotypic changes reflective of human disease (8) as well as reproducibility, often reported as being 100% successful in producing HCC in the appropriate sex and strain of rodent (9,18). Furthermore, DEN has been found to be primarily metabolized by and act locally on pericentral hepatocytes and these cells are known to proliferate through alterations in Wnt signaling, closely replicating the mechanism commonly observed in virally-induced human HCC (6,24–27). Prior research has shown that DEN-induced liver injury occurs in a dose-dependent manner, but achieving dose-dependent effects has typically required investigators to administer controlled doses themselves (18,19). The data from this study

show that survival and underlying liver disease can be manipulated by selecting rats on their weight at the initiation of an *ad libitum* DEN diet. This approach can allow investigators to create a high-throughput small animal model with predictable outcomes at a lower time and resource investment.

One of the main referenced limitations of the DEN model is the long latency of HCC development, reported in the literature as requiring as long as 50 weeks for tumors to develop (18). This study found that on average tumors took 98 days from the initiation of *ad libitum* DEN to reach detectable levels by imaging techniques. Moreover, while larger initial rat weight was found to have a favorable outcome on survival, no significant correlation was found between weight and tumor latency. These findings supofport the use of heavier rats for survival studies as they would allow for more experimental manipulation after the development tumors without having a considerable impact on the overall length of the study or time to tumor development.

The improved survival observed for larger rats may reflect differences in hepatocellular dysfunction supported by the finding of significantly increased liver cirrhosis associated with lower body weight. Prior research has shown that mammalian water consumption, including in the rat, is inversely related to body weight (20,21). With this knowledge, it's possible that the findings of increased hepatotoxicity observed in smaller rats are related to relative dose-dependent effects. While our data of DEN consumption in larger rats show no significant survival differences for that weight range, comparison to a smaller weight cohort may provide explanation for the observed outcome.

In addition to the characterization of the effect of initial body weight on survival, the current study compares a more clinically relevant technique of femoral TAE to previously reported carotid TAE in a rat model. Hepatic angiography via femoral catheterization has been previously reported in a rat model (16,17). Multiple studies demonstrate successful TAE performed via laparotomy (14,15). In recent years it has also been shown that selective hepatic embolization can be achieved through an endovascular approach without entering the peritoneum by cannulating the rat carotid artery (7,10). The present study demonstrates a technique that can be used with autochthonous tumors to achieve the same technical success and peri-procedural survival with a transfemoral approach. The reduced procedure time required for the femoral approach technique may facilitate increased throughput for studies of TAE in rat models and lessen the likelihood of complications associated with prolonged anesthesia and carotid manipulation. Based on our experience, the reduced procedure time may be related to both the ease of arterial isolation for access and the favorable course of arterial anatomy from the femoral approach as compared to the carotid. During multiple procedures in our study, carotid catheterization required careful extensive manipulation to direct the catheter away from the ascending portion of the aortic arch whereas celiac catheterization can be performed with relative ease via common femoral artery. Furthermore, by approaching the hepatic arteries from the common femoral artery, the proceduralist is able to leverage the straighter vascular course and improve ease of selective catheterization. Additionally, in cases where post-procedure arterial ligation is required, femoral artery ligation has been demonstrated and would offer a safer alternative to carotid ligation (16).

While this study has shown several advances for small animal modeling of HCC and TAE, there are important limitations. Firstly, incomplete data were available for several of the analyses presented. This is most apparent in our reduction from rats completing the diet to rats that were imaged and was due to the ongoing development of improved MR sequences early in the study. Secondly, the study applied a retrospective design without randomization and rats undergoing embolization via carotid approach were all from the smallest cohort which may influence ease of catheterization and were treated early in the study and as a result increased experience during the procedures for the group treated via femoral approach may have influenced outcomes. However, the operators had no prior experience in catheterization of femoral arteries in rats, and yet, the average procedure time was reduced by almost 1 hour. Further, all procedures were performed by fellowship-trained interventional radiologists and have not yet been consistently demonstrated by less experienced investigators so the generalizability of this technique remains to be determined. Finally, because larger rats in this study are also older, it remains uncertain if the differences detected are a function of size-related dose differences or age-related metabolic differences, though the outcome remains the same.

Overall, the findings from this study further characterize DEN-induced HCC and TAE in a rat model and provide methods for the refinement of future translational studies. By choosing larger animals for tumor induction, investigators can achieve improved survival while maintaining tumor induction for the purpose of survival studies at a fixed *ad libitum* concentration. The advancement of transfemoral arterial embolization in a small animal model allows for selective treatment of tumors and more closely mimics the techniques used in patients with reduced procedure times allowing higher throughput. Ultimately, this model will enable therapeutic advancements by serving as a reproducible small animal model of histologically-confirmed HCC and transfemoral embolization.

Supplementary Material

Refer to Web version on PubMed Central for supplementary material.

Acknowledgments

The authors would like to thank the Histology Core at the Abramson Family Cancer Research Institute for their contributions. Ryan M. Kiefer is a Howard Hughes Medical Institute – Society of Interventional Radiology Foundation Medical Research Fellow.

References

1. Forner A, Llovet JM, Bruix J. Hepatocellular carcinoma. Lancet. 2012; 379(9822):1245–55. Internet. Available from: http://dx.doi.org/10.1016/S0140-6736(11)61347-0. [PubMed: 22353262]
2. Llovet JM, Real MI, Montaña X, Planas R, Coll S, Aponte J, et al. Arterial embolisation or chemoembolisation versus symptomatic treatment in patients with unresectable hepatocellular carcinoma: a randomised controlled trial. Lancet (London, England). 2002; 359(9319):1734–9. Internet. Available from: http://www.ncbi.nlm.nih.gov/pubmed/12049862.
3. Brown KT, Do RK, Gonen M, Covey AM, Getrajdman GI, Sofocleous CT, et al. Randomized trial of hepatic artery embolization for hepatocellular carcinoma using doxorubicin-eluting microspheres compared with embolization with microspheres alone. J Clin Oncol. 2016; 34(17):2046–53. [PubMed: 26834067]

4. Prieto J, Melero I, Sangro B. Immunological landscape and immunotherapy of hepatocellular carcinoma. Nat Rev Gastroenterol Hepatol. 2015; 12(12):681–700. Internet. Available from: http://www.nature.com/nrgastro/journal/v12/n12/pdf/nrgastro.2015.173.pdf. [PubMed: 26484443]
5. Llovet J, Bruix J. Molecular targeted therapies in hepatocellular carcinoma. Hepatology. 2008; 48(4):1312–27. Internet. Available from: http://onlinelibrary.wiley.com/doi/10.1002/hep.22506/full. [PubMed: 18821591]
6. Arzumanyan, a, Reis, HM., Feitelson, M a. Pathogenic mechanisms in HBV- and HCV-associated hepatocellular carcinoma. Nat Rev Cancer. 2013;; 13(2):123–35. Internet. Available from:http://www.ncbi.nlm.nih.gov/pubmed/23344543%5Cnhttp://www.nature.com/nrc/journal/v13/n2/pdf/nrc3449.pdf. [PubMed: 23344543]
7. Gade TPF, Hunt SJ, Harrison N, Nadolski GJ, Weber C, Pickup S, et al. Segmental TAE in a Translational Rat Model of Hepatocellular Carcinoma. J Vasc Interv Radiol. 2015; 26(8):1–9. Internet. Available from: http://www.sciencedirect.com/science/article/pii/S1051044315001864. [PubMed: 25541442]
8. Groβ C, Steiger K, Sayyed S, Heid I, Feuchtinger A, Walch A, et al. Model matters: Differences in orthotopic rat hepatocellular carcinoma physiology determine therapy response to sorafenib. Clin Cancer Res. 2015; 21(19):4440–50. [PubMed: 25995341]
9. Newell P, Villanueva A, Friedman SL, Koike K, Llovet JM. Experimental models of hepatocellular carcinoma. J Hepatol. 2008; 48(5):858–79. [PubMed: 18314222]
10. Cho HR, Choi JW, Kim HC, Song YS, Kim GM, Son KR, et al. Sprague-Dawley rats bearing McA-RH7777 cells for study of hepatoma and transarterial chemoembolization. Anticancer Res. 2013 Jan; 33(1):223–30. [PubMed: 23267149]
11. Becher OJ, Holland EC. Genetically engineered models have advantages over xenografts for preclinical studies. Cancer Res. 2006; 66(7):3355–8. [PubMed: 16585152]
12. Falk P. Differences in vascular pattern between the spontaneous and the transplanted C3H mouse mammary carcinoma. Eur J Cancer Clin Oncol. 1982; 18(2):155–65. [PubMed: 7201391]
13. Zhang, W., Chen, HJ., Wang, ZJ., Huang, W., Zhang, LJ. Dynamic contrast enhanced MR imaging for evaluation of angiogenesis of hepatocellular nodules in liver cirrhosis in N-nitrosodiethylamine induced rat model. Eur Radiol. 2016. InternetAvailable from:http://link.springer.com/10.1007/s00330-016-4505-1
14. Ni, J., Xu, L., Wang, W., Huang, Q., Sun, H., Chen, Y. TAE combined with RNA interference targeting hypoxia-inducible factor-1α for hepatocellular carcinoma: a preliminary study of rat model. J Cancer Res Clin Oncol. 2016. InternetAvailable from:http://link.springer.com/10.1007/s00432-016-2237-x
15. Lee J, Gordon AC, Kim H, Park W, Cho S, Lee B, et al. Targeted multimodal nano-reporters for pre-procedural MRI and intra-operative image-guidance. Biomaterials. 2016; 109:69–77. Internet. Available from: http://linkinghub.elsevier.com/retrieve/pii/S0142961216304975. [PubMed: 27673597]
16. Ju S, McLennan G, Bennett SL, Liang Y, Bonnac L, Pankiewicz KW, et al. Technical Aspects of Imaging and Transfemoral Arterial Treatment of N1-S1 Tumors in Rats: An Appropriate Model to Test the Biology and Therapeutic Response to Transarterial Treatments of Liver Cancers. J Vasc Interv Radiol. 2009; 20(3):410–4. Internet. Available from: http://dx.doi.org/10.1016/j.jvir.2008.12.408. [PubMed: 19167243]
17. Thompson SM, Callstrom MR, Knudsen B, Anderson JL, Carter RE, Grande JP, et al. Development and preliminary testing of a translational model of hepatocellular carcinoma for MR imaging and interventional oncologic investigations. J Vasc Interv Radiol. 2012; 23(3):385–95. Internet. Available from: http://dx.doi.org/10.1016/j.jvir.2011.11.018. [PubMed: 22265247]
18. De Minicis S, Kisseleva T, Francis H, Baroni GS, Benedetti A, Brenner D, et al. Liver carcinogenesis: Rodent models of hepatocarcinoma and cholangiocarcinoma. Dig Liver Dis. 2013; 45(6):450–9. Internet. Available from: http://dx.doi.org/10.1016/j.dld.2012.10.008. [PubMed: 23177172]
19. Williams GM, Iatropoulos MJ, Jeffrey a M. Mechanistic basis for nonlinearities and thresholds in rat liver carcinogenesis by the DNA-reactive carcinogens 2-acetylaminofluorene and diethylnitrosamine. Toxicol Pathol. 2000; 28(18):388–95. [PubMed: 10862555]

20. Adolph EF. Quantitative Relations in the Physiological Constitutions of Mammals. Science (80-). 1949; 109(2841):579–85.
21. Holdstock TL. Body weight and water consumption in rats. Physiol Psychol. 1973; 1(1):21–3.
22. Laboratories, CR. [cited 2017 Feb 2] Wistar rat data sheets. 2017. InternetAvailable from: http://www.criver.com/products-services/basic-research/find-a-model/wistar-rat
23. Bedossa P, Poynard T. An algorithm for the grading of activity in chronic hepatitis C. The METAVIR Cooperative Study Group. Hepatology. 1996; 24:289–93. Internet. Available from: http://www.ncbi.nlm.nih.gov/pubmed/8690394. [PubMed: 8690394]
24. Sell S. Cellular origin of hepatocellular carcinomas. Semin Cell Dev Biol. 2002; 13:419–24. Internet. Available from: http://www.idealibrary.com. [PubMed: 12468242]
25. Font-Burgada J, Shalapour S, Ramaswamy S, Hsueh B, Rossell D, Umemura A, et al. Hybrid Periportal Hepatocytes Regenerate the Injured Liver without Giving Rise to Cancer. Cell. 2015; 162:766–79. [PubMed: 26276631]
26. Wang B, Zhao L, Fish M, Logan CY, Nusse R. Self-renewing diploid Axin2 cells fuel homeostatic renewal of the liver. Nature. 2015; 524:180–5. [PubMed: 26245375]
27. Choo SP, Tan WL, Goh BKP, Tai WM, Zhu AX. Comparison of hepatocellular carcinoma in Eastern versus Western populations. Cancer. 2016:3430–46.

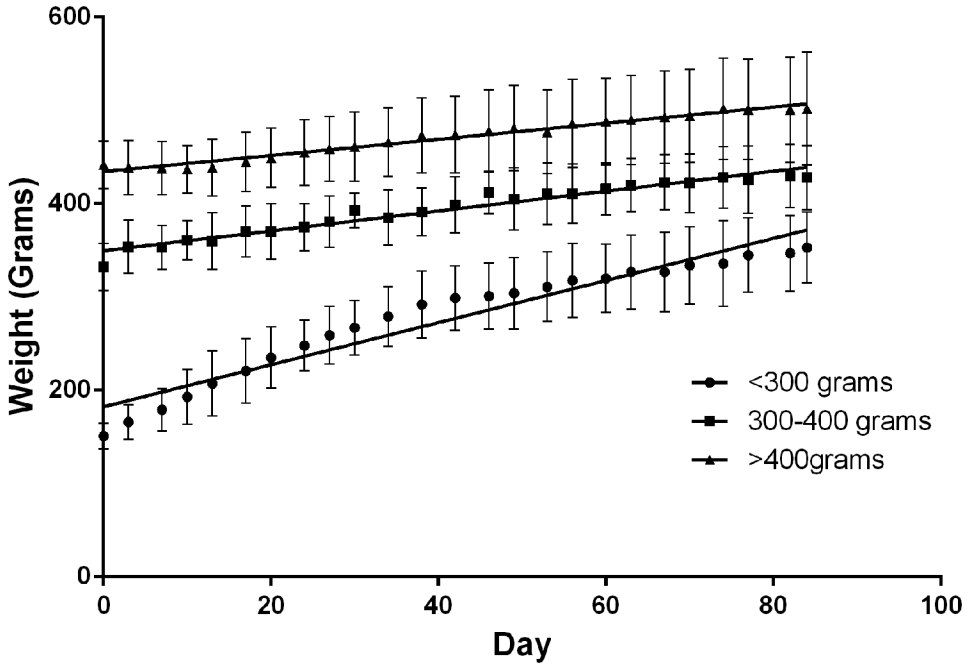

Figure 1.

Group weight trends throughout DEN diet. Each data point represents the average weight for all rats within the weight group on that day of the diet and are overlaid with a line of best fit. Error bars represent standard deviation.

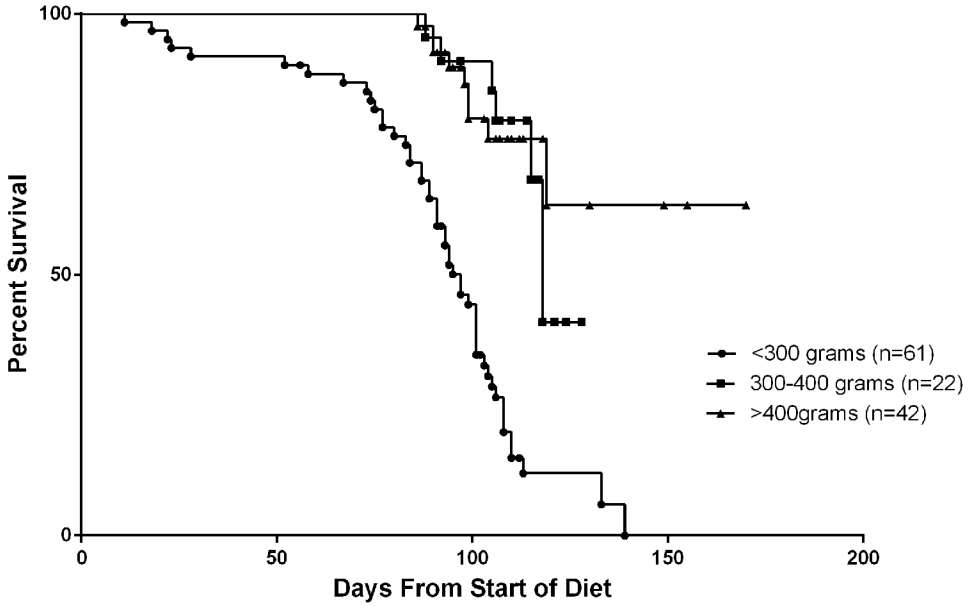

Figure 2.

Kaplan-Meier survival curve of rats by weight group. Rats were tracked until their natural death or were censored at their date of embolization if they were selected to undergo intervention.

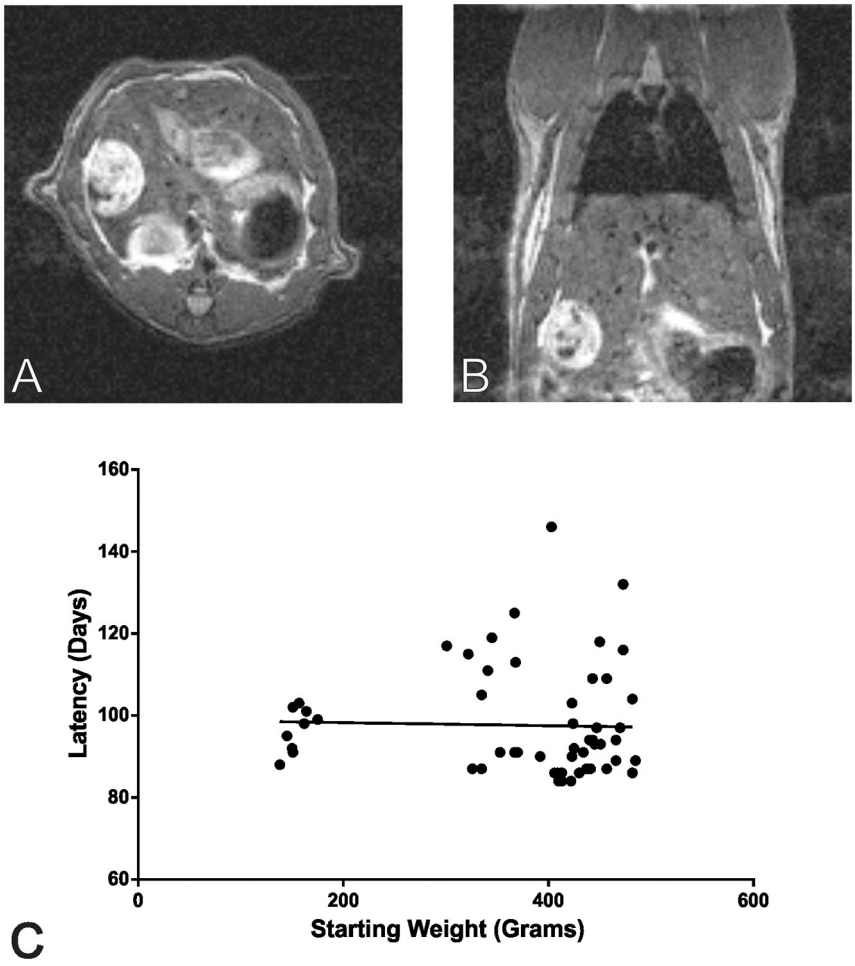

Figure 3.

Representative T2-weighted MR images for a rat showing a large tumor of HCC in the axial (Panel A) and coronal (Panel B) planes. Note that this tumor is the same one see in fluoroscopic images in Figure 5. Panel C shows a scatter plot of weight and tumor latency with overlaid line of best fit.

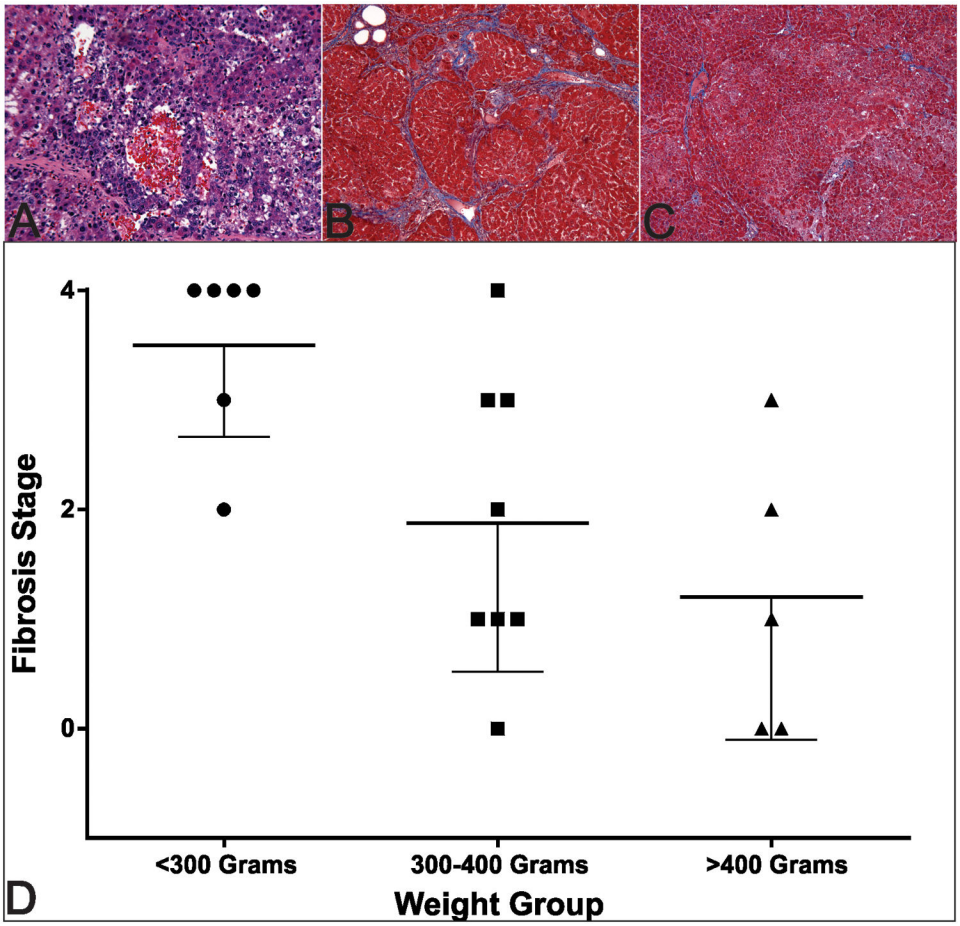

Figure 4.

Representative staining of the histologic changes observed in this model. Panel A shows representative H&E staining of HCC in this rat model. Panel B demonstrates marked liver fibrosis (Stage 4) seen in a <300g rat. Panel C shows less severe fibrosis (Stage 1) in a >400g rat compared with the smaller rat in panel B. Panel D demonstrates group fibrosis stages with a trend toward increasing severity at lower weight and a significantly increased fibrosis in the <300g group. The bold line represents the mean and lower error bars indicate standard deviation.

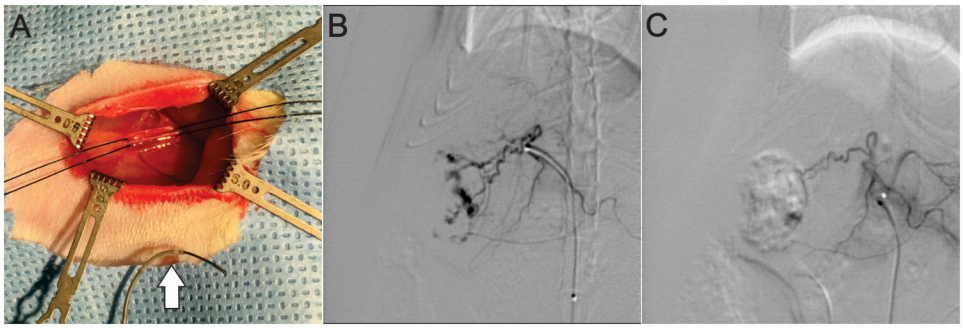

Figure 5.

(A) Intra-operative photo demonstrating the surgical field for the transfemoral arterial approach. 5-0 silk sutures can be seen positioned around the femoral artery as vessel loops. A 1.5F catheter with guidewire can be seen in the foreground for scale (white arrow). (B) Pre-embolization selective arteriogram showing superselective catheterization of the artery feeding the superior right lobe of the liver. (C) Post-embolization selective arteriogram demonstrating nearly complete embolization of large tumor as indicated by reduced contrast filling.

Table 1

Allocation of rats to the three study cohorts and number of rats used for each analysis within each cohort.

Total Rats	Cohorts	Diet Finished	Imaged	Treated
138 Male Wistar Rats	**<300g** (70 Rats)	54 Rats	13 Rats	13 Rats
	300-400g (23 Rats)	23 Rats	22 Rats	10 Rats
	>400g (45 Rats)	43 Rats	42 Rats	11 Rats

Table 2

Results from the carotid and femoral TAE approaches.

Embolization Approach	Technical Success	24-Hour Mortality	Procedure Time
Carotid Artery	10/13 Rats	1/10 Rats	127+/-24 minutes
Femoral Artery	20/21 Rats	2/20 Rats	71 +/-23 minutes